

# Imaging the Mott Insulator Shells using Atomic Clock Shifts

Gretchen K. Campbell,\* Jongchul Mun, Micah Boyd, Patrick Medley,  
Aaron E. Leanhardt,<sup>1</sup> Luis Marcassa,<sup>2</sup> David E. Pritchard, and Wolfgang Ketterle  
MIT-Harvard Center for Ultracold Atoms, Research Laboratory of Electronics  
and Department of Physics,

Massachusetts Institute of Technology, Cambridge, MA 02139, USA

<sup>1</sup> JILA, Boulder, CO 80309, USA

<sup>2</sup> Instituto de Fisica de Sao Carlos - University of São Paulo, Brazil

\*To whom correspondence should be addressed; E-mail: gcampbel@mit.edu.

**Microwave spectroscopy was used to probe the superfluid-Mott Insulator transition of a Bose-Einstein condensate in a 3D optical lattice. Using density dependent transition frequency shifts we were able to spectroscopically distinguish sites with different occupation numbers, and to directly image sites with occupation number  $n = 1$  to  $n = 5$  revealing the shell structure of the Mott Insulator phase. We use this spectroscopy to determine the onsite interaction and lifetime for individual shells.**

The Mott insulator transition is a paradigm of condensed matter physics. It describes how electron correlations can lead to insulating behavior even for partially filled conduction bands. However, this behavior requires a commensurable ratio between electrons and sites. If this condition on the density is not exactly fulfilled, the system will still be conductive. For neutral bosonic particles, the equivalent phenomenon is the transition from a superfluid to an insulator for commensurable densities. In inhomogeneous systems, as in atom traps, the condition

of commensurability no longer applies: for sufficiently strong interparticle interactions, it is predicted that the system should separate into Mott insulator shells with different occupation number, separated by thin superfluid layers [1, 2, 3].

The recent observation of the superfluid to Mott Insulator (MI) transition with ultracold atoms [4] has stimulated a large number of theoretical and experimental studies [see [5] and references therein]. Atomic systems allow for a full range of control of the experimental parameters including tunability of the interactions and defect-free preparation making them attractive systems for studying condensed matter phenomena. The Mott insulator phase in ultracold atoms has been characterized by studies of coherence, the excitation spectrum, and noise correlations [4, 6, 7]. Recently, using spin-changing collisions, lattice sites with two atoms were selectively addressed and the suppression of number fluctuations was observed [8].

The most dramatic new feature of the MI phase in ultracold atoms is the layered structure of the Mott shells, however until now this feature has not been directly observed. In this paper, we combine atoms in the Mott insulator phase with the high resolution spectroscopy used for atomic clocks, and use density dependent transition frequency shifts to spectroscopically resolve shells with occupancies from  $n = 1$  to 5 and directly image their spatial distributions.

Bosons with repulsive interactions in an optical lattice are accurately described by the Hamiltonian [9, 1],

$$\hat{H} = -J \sum_{\langle i,j \rangle} \hat{a}_i^\dagger \hat{a}_j + \frac{1}{2} U \sum_i \hat{n}_i (\hat{n}_i - 1) + \sum_i (\epsilon_i - \mu) \hat{n}_i, \quad (1)$$

where the first two terms are the usual Hamiltonian for the Bose-Hubbard model and the last term adds in the external trapping potential, and where  $J$  is the tunneling term between nearest neighbors,  $\hat{a}_i^\dagger$  and  $\hat{a}_i$  are the boson creation and destruction operators at a given lattice site,  $U = (4\pi\hbar^2 a/m) \int |w(x)|^4 d^3x$  is the repulsive onsite interaction, where  $m$  is the atomic mass,  $a$  is the s-wave scattering length and  $w(x)$  is the single particle Wannier function localized to

the  $i^{th}$  lattice site, and  $\hat{n}_i = \hat{a}_i^\dagger \hat{a}_i$  is the number operator for bosons at site  $i$ . The last term in the hamiltonian is due to the external trapping confinement of the atoms, where  $\epsilon_i = V_{ext}(r_i)$  is the energy offset at the  $i$ th site due to the external confinement and  $\mu$  is the chemical potential.

The behavior of this system is determined by the ratio of  $J/U$ . For low lattice depths, the ratio is large and the system is superfluid. For larger lattice depths, the repulsive onsite energy begins to dominate, and the system undergoes a quantum phase transition to a MI phase. For deep lattices the atoms are localized to individual lattice sites with integer filling factor  $n$ . This filling factor varies locally depending on the local chemical potential  $\mu_i = \mu - \epsilon_i$  as

$$n = Mod(\mu_i/U), \quad (2)$$

and decreases from the center to the edge of the trap.

To prepare the atoms in the Mott insulating phase, a  $^{87}\text{Rb}$  Bose-Einstein condensate was first created in the the  $|F = 1, m_F = -1\rangle$  state using a combination of a Ioffe-Pritchard magnetic trap and an optical dipole trap. The optical trap was oriented perpendicular to the long axis of the magnetic trap, creating a more isotropic trapping potential which was better matched to the optical lattice. The laser beam for the optical trap had a  $1/e^2$  waist of  $\approx 70 \mu\text{m}$ , and was retro-reflected. However, the polarization of the retro-reflected beam was rotated such that the interference between the two beams had minimal contrast. The resulting trap had radial (axial) trap frequencies of  $\omega = 2\pi \times 70$  (20) Hz, where the axial direction is now parallel to the optical trap. A 3D optical lattice was created by adding two additional retro-reflected laser beams derived from the same laser at  $\lambda = 1064 \text{ nm}$ . The lattice was adiabatically ramped up by rotating the polarization of the retro-reflected optical trapping beam to increase the interference contrast along that axis and by increasing the laser power in the other two axes. The lattice depth was increased using an exponential ramp with a 40 ms time constant. All three beams were linearly polarized orthogonal to each other and had different frequency detunings generated

using acousto-optic modulators. The lattice depth was up to  $40 E_{rec}$ , where  $E_{rec} = \hbar^2 k^2 / (2m)$  and  $k = 2\pi/\lambda$  is the wavevector of the lattice. At  $40 E_{rec}$  the lattice trap frequency at each site was  $\omega_{lat} = 2\pi \times 25$  kHz, and the external trap frequencies increased to  $\omega = 2\pi \times 110$  (30) Hz in the radial (axial) direction.

Zeeman shifts and broadening of the clock transition from the  $F = 1$  to the  $F = 2$  state were avoided by using a two photon transition between the  $|1, -1\rangle$  and the  $|2, 1\rangle$  state, where at a magnetic bias field of  $\sim 3.23$  G both states have the same first order Zeeman shift [10]. The two photon pulse was composed of one microwave photon at a fixed frequency of 6.83 GHz, and one rf photon at a frequency of around 1.67 MHz. The pulse had a duration of 100 ms, and when on resonance the fraction of atoms transferred to the  $|2, 1\rangle$  state was less than 20%. After the pulse, atoms in the  $|2, 1\rangle$  state were selectively detected with absorption imaging using light resonant with the  $5^2S_{1/2}|2, 1\rangle \rightarrow 5^2P_{3/2}|3, 1\rangle$  transition. For observing the spatial distribution of the Mott shells, the atoms were imaged in trap. For recording spectra, the atoms were released from the trap and imaged after 3 ms of ballistic expansion in order to reduce the column density

When the two photon spectroscopy is performed on a trapped condensate without a lattice, the atoms transferred to the  $|2, 1\rangle$  state have a slightly different mean field energy due to the difference between the  $a_{21}$  and  $a_{11}$  scattering lengths, where  $a_{21}$  is the scattering length between two atoms in states  $|2, 1\rangle$  and  $|1, -1\rangle$ , and  $a_{11}$  is the scattering length between two atoms in the  $|1, -1\rangle$  state. This difference in the scattering lengths leads to a density dependent shift to the resonance frequency  $\Delta\nu \propto \rho(a_{21} - a_{11})$ , where  $\rho$  is the condensate density [10]. This collisional shift is commonly referred to as the ‘clock’ shift [11] due to its importance in atomic clocks, where cold collisions currently limit the accuracy [12, 13]. When performed on a condensate with peak density  $\rho_0$  in a harmonic trap, in the limit of weak excitation, the line shape for the

2-photon resonance is given by [14]:

$$I(\nu) = \frac{15h(\nu - \nu_0)}{4\rho_0\Delta E} \sqrt{1 - \frac{h(\nu - \nu_0)}{\rho_0\Delta E}}, \quad (3)$$

with the mean field energy difference

$$\Delta E = \frac{\hbar^2}{\pi m} (a_{21} - a_{11}). \quad (4)$$

In the case of  $^{87}\text{Rb}$ ,  $a_{21}(a_{11}) = 5.19$  (5.32) nm [15]. Both the frequency shift and the linewidth increase with the condensate density. As the lattice is ramped on, the peak density of the condensate in a given lattice site increases as

$$\rho_0(r) = \left( \mu - \frac{1}{2} m \omega_{\text{trap}}^2 r^2 \right) 1/U, \quad (5)$$

where  $\omega_{\text{trap}}$  is the external trap frequency for the combined magnetic and optical trap, and using the Thomas Fermi approximation  $\mu$ , the chemical potential is given by

$$\mu = \left( \frac{15 (\lambda/2)^3 m^{3/2} N U \omega_{\text{trap}}^3}{16 \sqrt{2\pi}} \right)^{2/5}, \quad (6)$$

where  $N$  is the total atom number. For low lattice depths the system is still a superfluid, delocalized over the entire lattice. However, the two-photon resonance line is shifted and broadened due to the increased density, with the center of the resonance at  $\nu = \nu_0 + 2\rho_0\Delta E/3h$ . For deep lattices in the MI regime the repulsive onsite interaction dominates, number fluctuations are suppressed, and each lattice site has a sharp resonance frequency determined by the occupation number in the site. The separation between the resonance frequencies for the  $n$  and  $n - 1$  MI phases is given by

$$\delta\nu = \frac{U}{\hbar} (a_{21} - a_{11}) / a_{11}. \quad (7)$$

The linewidth of the resonances is no longer broadened by the inhomogeneous density and should be limited only by the bandwidth of the two photon pulse.

Fig. 1 shows the transition from a broadened resonance to several sharp lines as the lattice depth was increased. At a lattice depth of  $V = 5 E_{rec}$ , the line was broadened and the line center was shifted slightly due to the increased density. At  $V = 10 E_{rec}$ , the line was shifted and broadened further, and in addition the line shape became asymmetric as the atom number in lattice sites with small occupation was squeezed. For deeper lattice depths the system underwent a phase transition to a MI phase and discrete peaks appeared corresponding to MI phases with different filling factors, and for  $V = 35 E_{rec}$ , MI phases with occupancies of up to 5 were observed.

When the lattice depth was increased inside the MI regime (from  $V = 25 E_{rec}$  to  $35 E_{rec}$ ), the separation between the resonance peaks increased presumably due to the larger onsite interaction energy as the lattice trap was increased. As given in Eq. (7), the separation between the peaks provides a direct measurement of the onsite interaction energy  $U$ . As shown in Fig. 2a, our results are in good agreement with calculated values of  $U$ . Fig. 2b shows that although the separation between the  $n = 1, 2$  and 3 peaks is approximately constant, for higher filling factors the separation between the peaks decreases; the effective onsite interaction energy becomes smaller for higher filling factors. This shows that for low occupation numbers the atoms occupy the ground state wavefunction of the lattice site, whereas for larger occupation numbers, the repulsive onsite interaction causes the wavefunction to spread out lowering the interaction energy. From a variational calculation of the wavefunction similar to [16], we find the onsite energy for the  $n = 5$  shell should be  $\approx 20\%$  smaller than that for the  $n = 1$  shell, is in agreement with the measured value shown in Fig. 2b.

The peaks for the different occupation numbers were spectrally well separated. Therefore, on resonance, only atoms from a single shell were transferred to the  $|2, 1\rangle$  state. An image of these atoms (without any time-of-flight) shows the spatial distribution of this shell. Fig. 3b, shows absorption images for  $n = 1 - 5$  shells. As predicted [1], the  $n = 1$  MI phase appears

near the outer edge of the cloud. For larger  $n$ , the radius of the shell decreases, and the  $n = 5$  sites form a core in the center of the cloud. The expected radius for each shell was obtained from Eq. 2 using the measured values for the onsite interaction. The observed radii were in good agreement, except for the  $n = 1$  shell which may have been affected by anharmonicities in the external trap. Absorption images taken with rf frequencies between the peaks show a small signal, which may reflect the predicted thin superfluid layers between the insulating shells, however this needs to be studied further. The expected absorption image of a shell should show a column density with a flat distribution in the center and raised edges. However due to limitations (resolution and residual fringes) in our imaging system, these edges were not resolved.

Since we were able to address the different MI phases separately, the lifetime for each shell could be determined. For this, the atoms were first held in the lattice for a variable time  $\tau$  before applying the 100 ms two-photon pulse. For the  $n = 1$  MI phase, ignoring technical noise, the lifetime should only be limited by spontaneous scattering from the lattice beams. Even for the deepest lattices, the spontaneous scattering rate is  $< 10^{-2}$  Hz. For the  $n = 2$  MI phase the lifetime is limited by dipolar relaxation, which for  $^{87}\text{Rb}$  is slow with a rate  $< 10^{-2}$  Hz. For sites with  $n \geq 3$  the lifetime is limited by 3-body recombination with a rate  $\gamma n(n-1)(n-2)$  [17] with  $\gamma = 0.026$  Hz for our parameters. This gives 3-body lifetimes of  $\tau_{3B} = 6.2$  s, 1.6 s, and 0.6 s for the  $n = 3, 4,$  and  $5$  MI phases respectively. This calculation of  $\gamma$  assumes for the density distribution the ground state of the harmonic oscillator potential, so for higher filling factors the actual lifetime could be higher. In Fig. 4, we show relative populations as a function of the hold time and derive lifetimes as  $\tau \approx 1$  s, 0.5 s, and 0.2 s for the  $n = 3, 4,$  and  $5$  MI phases, this is shorter than predicted which is possibly due to secondary collisions. For  $n = 1$  and  $2$ , lifetimes of over 5 s were observed.

In this work we have used an atomic clock transition to characterize the superfluid - Mott insulator transition. This demonstrates the power of applying precision methods of atomic

physics to problems of condensed matter physics. Exploiting atomic clock shifts, we could distinguish sites according to their occupation number. This allowed us to directly image the Mott insulator shells with filling factors  $n = 1 - 5$ , and to determine the onsite interaction and lifetime as a function of  $n$ .

In the future, this method can be used to measure the number statistics as the system undergoes the phase transition. One would expect that the spectral peaks for higher occupation number become pronounced only at higher lattice depth — an indication of this can be seen already in Fig. 1. For low lattice depths, the tunneling rate is still high, but one can suddenly increase the lattice depth and freeze in populations [18], which can then be probed with high resolution spectroscopy. Fluctuations in the atom number could identify the superfluid layers between the Mott shells. In addition, by applying a magnetic gradient across the lattice, tomographic slices could be selected, combining full 3D resolution with spectral resolution of the site occupancy. The addressability of individual shells could be used to create systems with only selected occupation numbers (e.g. by removing atoms in other shells). Such a preparation could be important for the implementation of quantum gates for which homogenous filling is desirable. For atoms other than rubidium, atomic clock shifts are much larger, e.g. for sodium by a factor of 30. Therefore, it should be easier to resolve the Mott insulator shells, unless the collisional lifetime of the upper state of the clock transition sets a severe limit to the pulse duration [19].

## References

- [1] D. Jaksch, C. Bruder, J. I. Cirac, C. W. Gardiner, P. Zoller, *Phys. Rev. Lett.* **81**, 3108 (1998).
- [2] G. G. Batrouni, R. T. Scalettar, G. R. Zimanyi, *Phys. Rev. Lett* **65**, 1765 (1990).



- [3] B. D. Marco, C. Lannert, S. Vishveshwara, T. C. Wei, *Phys. Rev. A* **71**, 063601 (2005).
- [4] M. Greiner, O. Mandel, T. Esslinger, T. W. Hänsch, I. Bloch, *Nature* **415**, 39 (2002).
- [5] I. Bloch, *Nature Physics* **1**, 23 (2005).
- [6] T. Stöferle, H. Moritz, C. Schori, M. Köhl, T. Esslinger, *Phys. Rev. Lett.* **92**, 130403 (2004).
- [7] S. Fölling, *et al.*, *Nature* **434**, 481 (2005).
- [8] F. Gerbier, S. Fölling, A. Widera, O. Mandel, I. Bloch, *Phys. Rev. Lett.* **96**, 090401 (2006).
- [9] M. P. A. Fisher, P. B. Weichman, G. Grinstein, D. S. Fisher, *Phys. Rev. B* **40**, 546 (1989).
- [10] D. M. Harber, H. J. Lewandowski, J. M. McGuirk, E. A. Cornell, *Phys. Rev. A* **66**, 053616 (2002).
- [11] K. Gibble, S. Chu, *Phys. Rev. Lett.* **70**, 1771 (1993).
- [12] C. Fertig, K. Gibble, *Phys. Rev. Lett.* **85**, 1622 (2000).
- [13] Y. Sortais, *et.al*, *Phys. Scr* **T95**, 50 (2001).
- [14] J. Stenger, *et al.*, *Phys. Rev. Lett.* **82**, 4569 (1999).
- [15] E. G. M. van Kempen, S. J. J. M. F. Kokkelmans, D. J. Heinzen, B. J. Verhaar, *Phys. Rev. Lett* **88**, 093201 (2002).
- [16] G. Baym, C. J. Pethick, *Phys. Rev. Lett.* **76**, 6 (1996).
- [17] M. W. Jack, M. Yamashita, *Phys. Rev. A* **67**, 033605 (2005).
- [18] M. Greiner, O. Mandel, T. W. Hänsch, I. Bloch, *Nature* **419**, 51 (2002).
- [19] This work was supported by NSF.

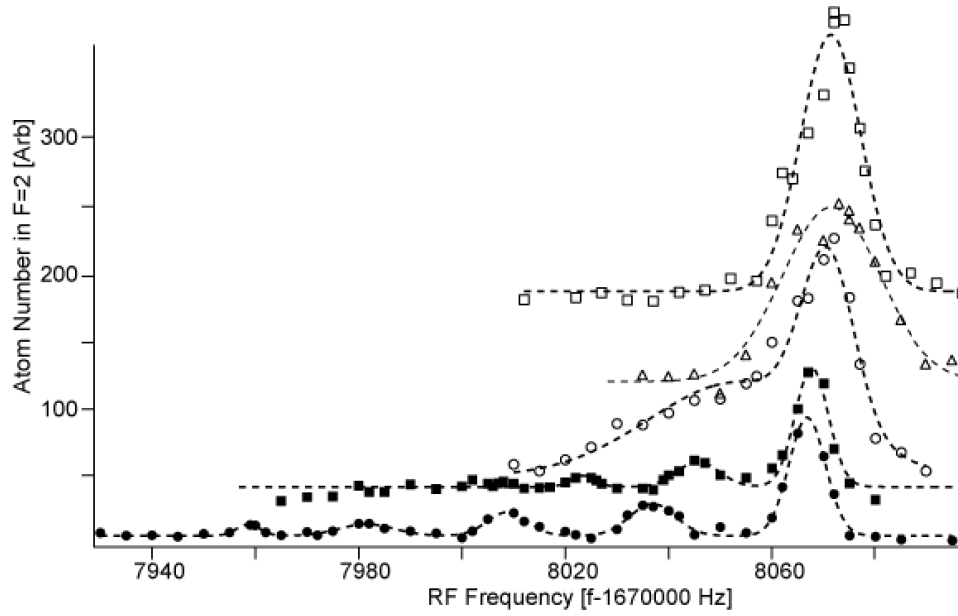


Figure 1:

**Fig. 1.** Two-photon spectroscopy across the superfluid to Mott insulator transition. Spectra for 3D lattice depths of  $0 E_{rec}$  (open squares),  $5 E_{rec}$  (open diamonds),  $10 E_{rec}$  (open circles),  $25 E_{rec}$  (solid squares), and  $35 E_{rec}$  (solid circles) are shown. The spectra are offset for clarity. The shift in the center of the  $n=1$  peak as the lattice depth is increased is due to the differential AC Stark shift from the lattice. The dotted lines show gaussian fits of the peaks.

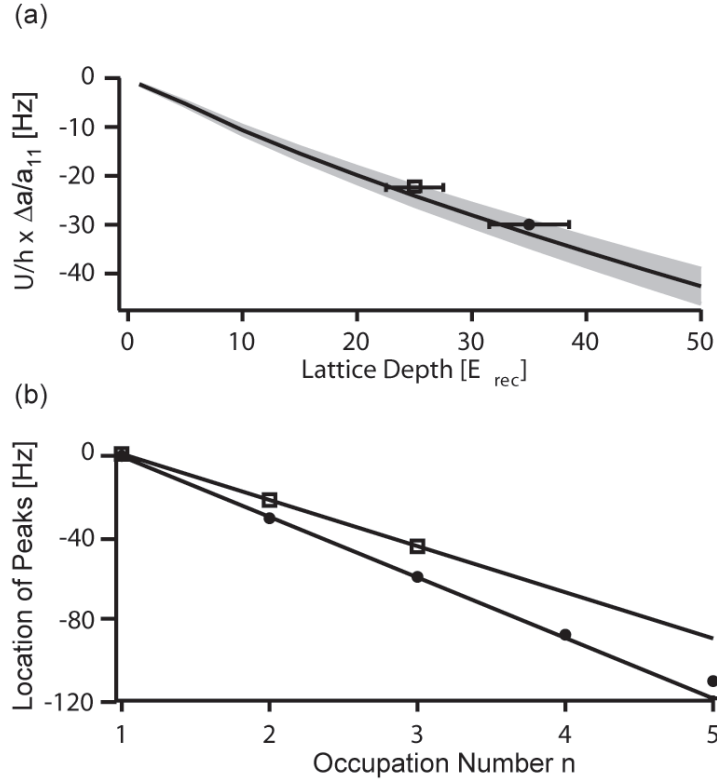


Figure 2:

**Fig. 2.** Probing the onsite interaction energy. (a) The separation between the  $n = 1$  and  $n = 2$  peaks is shown for lattice depths of  $V = 25 E_{rec}$  (squares) and  $V = 35 E_{rec}$  (circles). As the lattice depth was increased the separation increased from 22(1) Hz to 30(1) Hz. The shaded area gives the expected value determined from a band structure calculation, including the uncertainty in the scattering lengths. The uncertainty in the measured separation is indicated by the size of the points. (b) Location of resonances for all MI phases relative to the  $n = 1$  phase for  $V = 25 E_{rec}$  and  $V = 35 E_{rec}$ . For low site occupation ( $n = 1, 2, 3$ ), the separation between the resonances is approximately constant, implying constant on-site interaction energy  $U$ . For  $V = 35 E_{rec}$ , the separation between the  $n = 4$  and 5 peaks was 22(2) Hz, a 27% decrease from the 30(1) Hz separation between the  $n = 1$  and 2 peaks. The slope of the lines is fit to the separation between the  $n = 1$  and 2 peaks.

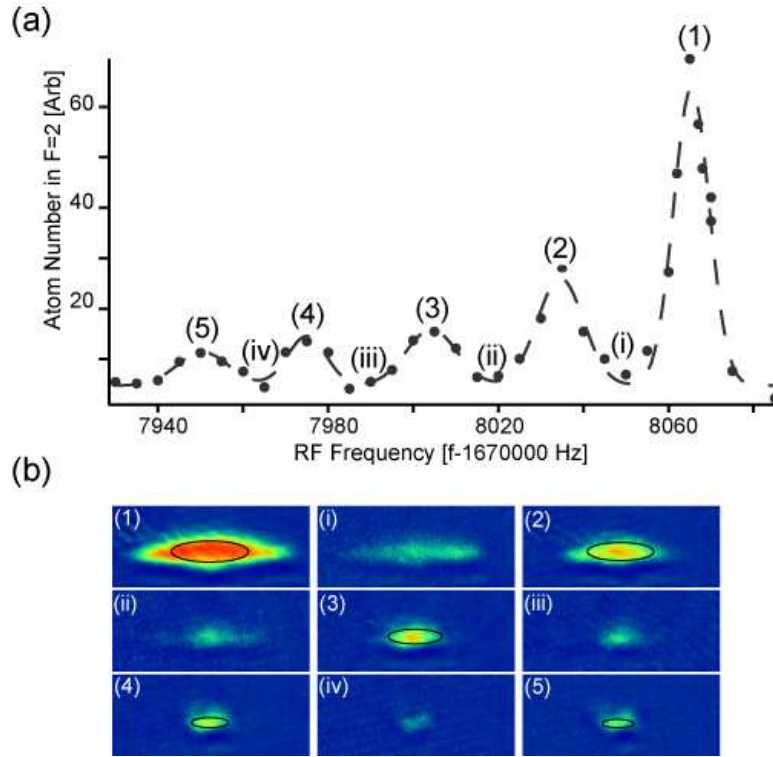


Figure 3:

**Fig. 3.** Imaging the shell structure of the Mott insulator. (a) Spectrum of the Mott insulator at  $V = 35 E_{rec}$ . (b) Absorption images for decreasing rf frequencies. Images 1, 2, 3, 4 and 5 were taken on resonance with the peaks shown in (a) and display the spatial distribution of the  $n = 1-5$  shells. The solid lines show the predicted contours of the shells. Absorption images taken for rf frequencies between the peaks (images *i*, *ii*, *iii* and *iv*) show a much smaller signal. The field of view was  $185 \mu\text{m} \times 80 \mu\text{m}$ .

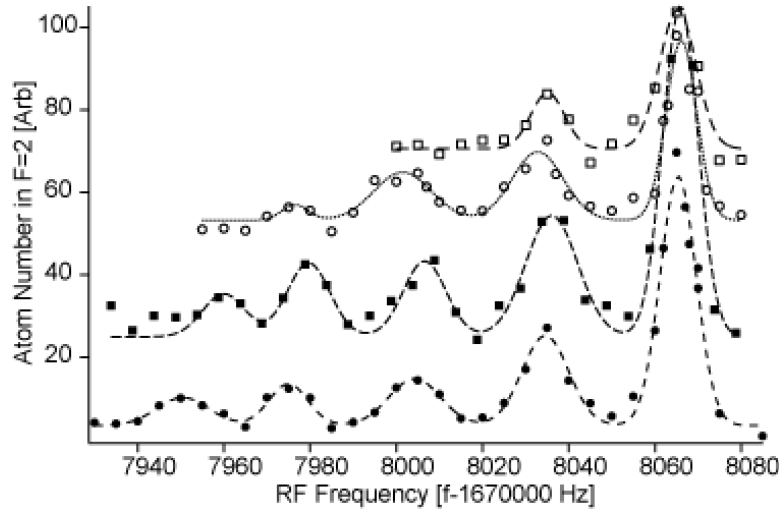


Figure 4:

**Fig. 4.** Lifetime of individual MI shells. The lifetime for each MI phases can be measured independently by adding a hold time before applying the two photon pulse. Spectra are shown for hold times of 0 ms (filled circles), 100 ms (filled squares), 400 ms (open circles), 2000 ms (open squares). The lattice depth was  $V = 35 E_{rec}$  except for the 100 ms hold time, for which it was  $V=34 E_{rec}$ . The lines show gaussian fits to the peaks, and the spectra were offset for clarity.